AIAA JOURNAL
Vol. 32, No. 11, November 1994

Analysis and Test Correlation of Spacecraft Structures Using Dynamic Parameter Sensitivities

Srinivas Kodiyalam* and Pi-Jen Kao†
General Electric Corporate Research and Development Center, Schenectady, New York 12301
and
George Wang‡
Martin Marietta Astro Space, Princeton, New Jersey 08543

A synergistic approach, using both test measurements and analytical model predictions, is outlined to accurately identify the dynamic characteristics of structural systems, more specifically, spacecraft systems. The test correlated dynamic model of the spacecraft structural system is in turn used for performing a detailed loads analysis of the coupled launch vehicle-spacecraft system, which verifies the integrity of spacecraft. A combination of error location procedure and parameter estimation method is used in correlating the finite element analytical model predictions with test measurements. Both frequency and mode shape correlations are imposed as direct requirements in the parameter estimation problem. The parameter estimation problem itself is solved using dynamic parameter sensitivities and mathematical programming methods. An interplanetary spacecraft design along with its test measurements is used in validating the proposed approach.

I. Introduction

THE development of an accurate analytical model for a structural system, more specifically, a spacecraft system, is a fundamental requirement of engineering analysis. Comparison of the analytical model responses with the test measurements is frequently used as a measure of the model's accuracy. Very often, the analytical model does not produce the dynamic parameters (frequencies, mode shapes, ..., etc.) that adequately match with the test results and, therefore, an iterative cycle is necessary to adjust the analytical model with the test results. The analytical model predictions may differ from the actual structural behavior due to several reasons, including manufacturing tolerances, errors in modeling connections and boundary conditions, differences in material properties (especially for complex material systems), as well as nonlinear effects (see Fig. 1). Test measurements can also be inaccurate due to noisy measurements, insufficient measurement degrees of freedom, and inaccuracies associated with the curve fitting process. With increasingly complex spacecraft systems, the model tuning becomes virtually intractable using manual trial and error approaches, hence the need for systematic identification approaches.

Analytical model and test correlation procedures for system responses, also referred to as system identification methods, have been a topic of research for over two decades.[1–3] In a broad sense, these methods adjust the model by varying the parameters of the mathematical model in such a way that the model characteristics approach the characteristics of the system under study in some predetermined sense. Apart from directly tuning the analytical model based on measured test data, research has also focused on optimal modification of the measured mode shapes and subsequent use of these "true" measured mode shapes for correlation with the analytical model dynamic parameters.[4] In Ref. 5, a method is outlined to calculate the dynamic parameter (frequency and mode shape) sensitivities with respect to the structural model parameters such as elements of the mass and stiffness matrix. The sensitivities are then used to adjust the mass and stiffness characteristics of the model to match the model predictions with the measured data. The advantages of this approach are the applicability to large-scale structures and a computationally efficient way of recomputing the dynamic parameters.

An important aspect of the overall analysis and test correlation process is the ability to accurately identify the erroneous regions of the analytical model.[6] The model correlation process is significantly more robust when implemented on these identified local error regions.

In this paper, the analysis and test correlation of the dynamic characteristics of the structure is accomplished using a combination of mathematical programming methods and dynamic parameter sensitivities with respect to relevant structural parameters. Mathematical programming methods, along with design sensitivity coefficients, have been used in the past to solve the model correlation problem.[7,8] A performance index is minimized subject to bounds on the design variables. However, in the formulation presented here, a constrained minimization formulation is adopted, with explicit requirements on both frequencies and mode shapes of the structure. The systematic identification method reported here consists of three main steps, including: 1) location of error in the analytical model through comparing analysis and test measured mode shapes and using energy checks; 2) selection of relevant structural parameters that influence local regions of error, identified in step 1, using the analyst's judgement; and 3) estimation of structural parameters, identified in step 2, using mathematical programming methods.

Several unique aspects of this work include the use of high-level structural parameters that can be directly related to the drawings:

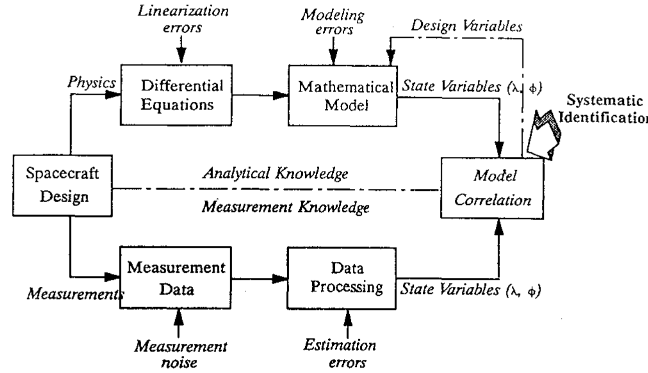

Fig. 1 Mathematical model correlation.

Received Oct. 12, 1993; presented as Paper 94-1502 at the AIAA/ASME/ASCE/AHS/ASC 35th Structures, Structural Dynamics, and Materials Conference, Hilton Head, SC, April 18–20, 1994; revision received May 31, 1994; accepted for publication May 31, 1994.

*Staff Mechanical Engineer, Engineering Mechanics Laboratory. Senior Member AIAA.

†Staff Mechanical Engineer, Engineering Mechanics Laboratory. Member AIAA.

‡Staff Mechanical Engineer, Spacecraft Analysis Group. Member AIAA.

as design variables in the analysis and test correlation process as against entries in the stiffness and mass matrices, by use of analysis and test-mode shape cross-orthogonality requirements as an integral part of the parameter estimation problem formulation, and by the use of mode shape sensitivities in the solution of the parameter estimation problem, apart from the frequency derivatives. In addition, robust approximations to the objective and constraint functions of the parameter estimation problem are used to minimize the computational time required for the iterative modal analysis and test correlation process. A Martin Marietta interplanetary spacecraft design, along with its modal test measurements, is used in validating the proposed methodology.

II. Analytical Model Correlation Criteria

The analytical model of a structural system is considered to be a good representation of the structure provided the dynamic parameters of the model are in good agreement with the measured data. In this work, the analysis and test mode shapes self- and cross-orthogonality requirements, along with their frequency correlation, are used as the criteria for judging the degree of correlation. Modal effective weight checks using both the analysis and test mode shapes are also performed to ensure the dominant modes have been correlated.

A. Self-Orthogonality Check

The self-orthogonality check is performed to assess the validity of the measured mode shapes by checking their orthogonality through the analytical mass matrix. Given a measured mode shape matrix Φ_T of size (n, m) and $(n > m)$, a symmetric positive definite matrix M of size (n, n) corresponding to the analytical model mass matrix, the self orthogonality of the mass normalized test mode shapes with respect to the mass matrix is given by

$$[C_s] = [\Phi_T]^t[M][\Phi_T] = [I] \tag{1}$$

where, the measured mode shapes Φ_T are mass normalized as follows:

$$[\Phi_T] = \tilde{\Phi}_T\left(\tilde{\Phi}_T^t M \tilde{\Phi}_T\right)^{-1/2} \tag{2}$$

where $\tilde{\Phi}_T$ is the measured mode shape matrix before normalization. The self-orthogonality matrix C_s should be a unit matrix if the measured modes are mass normalized and orthogonal with respect to the analytical model mass matrix. However, since it is normally not possible to have measurements corresponding to every degree of freedom of the analytical model, the orthogonality check is generally performed with a reduced size mass matrix M_{aa} (the reduction process is briefly described in Sec. III). Therefore, it is reasonable to consider diagonal elements of matrix C_s in excess of $|0.9|$ as close to unity and off-diagonal terms below $|0.05|$ as small.

B. Cross-Orthogonality Check

The cross-orthogonality check provides a way of checking the correlation between the analytical model mode shapes Φ_A and the measured mode shapes Φ_T, thereby identifying the analysis mode shape that matches with the measured mode shape. Given a measured mode shape matrix Φ_T of size (n, m), a symmetric positive definite matrix M of size (n, n) corresponding to the analytical model mass matrix, and the analytical model mode shape matrix Φ_A of size (n, m), the cross orthogonality between the analysis and test mode shapes with respect to the mass matrix is given by

$$[C_x] = [\Phi_A]^t[M][\Phi_T] \tag{3}$$

The elements of the cross-orthogonality matrix C_x represents the degree of correlation between the analytical model and the measured mode shapes. A unity matrix for C_x would mean a precise correlation between the analytical and measured mode shapes. A criterion used in this work for deciding on the convergence of the systematic identification method is the diagonal terms of the cross-orthogonality matrix to be greater than $|0.90|$ and the off-diagonal terms to be less than $|0.10|$.

C. Modal Effective Weight

The modal effective weight (MEW) provides an estimate of the participation of a vibration mode, in terms of the load it will cause on the structure, when excited. The more MEW in a mode, the more load it will input to the structure when excited. Therefore, it is necessary to ensure that modes with high MEW be identified and correlated with test measurements. The MEW calculation is given by

$$\text{MEW} = \text{Diag}([\Phi_T]^t[M][\Phi_{\text{RB}}])^2 \tag{4}$$

where $[\phi_{\text{RB}}]$ is the rigid body matrix. In this work, all of the vibration modes that have a ratio of MEW to the spacecraft physical weight over 5% are retained for the correlation process.

III. Reduction of the Analytical Model Stiffness and Mass Matrices

In the case of structural systems, like the spacecraft systems, the number of measurement degrees of freedom is considerably less compared to the physical degrees of freedom. Therefore, the analytical model mode shapes cannot be directly compared to the test measurements. Two possible solutions to this incompatability in the measurement and analytical model degrees of freedom exist: 1) expansion of the measured mode shapes to the full physical degrees of freedom using the analytical model mass and stiffness matrices, and 2) reduction of the analytical model mass and stiffness matrices to the measurement degrees of freedom. In this work, the latter solution is adopted, and the Guyan reduction[9] and improved reduction procedure[10] are investigated to reduce the stiffness and mass matrices.

With Guyan reduction (or static condensation), the unconstrained structural coordinates are partitioned into the analysis set u_a and the dependent set u_d. The transformation matrix Ψ is a function of only the structural stiffness matrix and is given by

$$\begin{Bmatrix} u_d \\ u_a \end{Bmatrix} = [\Psi]\{u_a\} \tag{5}$$

and

$$\Psi = \begin{bmatrix} -[K_{dd}]^{-1}[K_{da}] \\ [I_{aa}] \end{bmatrix}$$

The reduced stiffness and mass matrices are given by

$$\begin{aligned} K_{aa} &= [\Psi]^t[K][\Psi] \\ M_{aa} &= [\Psi]^t[M][\Psi] \end{aligned} \tag{6}$$

Guyan reduction produces an exact reduction of the stiffness matrix, although only an approximate reduction of the mass matrix, if any degree of freedom with mass is not included in the analysis set. For complex spacecraft models with smeared masses, this approximate reduction of the mass matrix may result in unacceptably large errors.

The improved reduction procedure is basically an extension of the Guyan reduction and explicitly includes a static approximation for the dynamic/mass terms discarded in the Guyan reduction procedure. With the improved reduction procedure, the transformation matrix Ψ_{IRS} is given by

$$\Psi_{\text{IRS}} = \begin{bmatrix} \Psi_{\text{static}} + \Psi_{\text{dynamic}} \\ [I_{aa}] \end{bmatrix} \tag{7}$$

where

$$\Psi_{\text{static}} = -[K_{dd}]^{-1}[K_{da}]$$

$$\Psi_{\text{dynamic}} = K_{dd}^{-1}[M_{da} + M_{dd}\Psi_{\text{static}}]M_{aa}^{-1}K_{aa}$$

Clearly, the accuracy of the Guyan reduction and the improved reduction procedures depends on the proper choice of the analytical model degrees of freedom u_a retained for the normal modes analysis. In this work, the analyses degrees of freedom correspond one-to-one with the measurement degrees of freedom.

IV. Energy Checks for Location of Modeling Errors

Several of the reported researches in analysis/test correlation procedures have modified the complete structure to match a limited set of measurements. A major drawback of this is that portions of the structure that were originally correct might have been changed to match the limited test data. Therefore, it is essential that erroneous regions of the analytical model be first identified and model parameters that affect these regions be tailored to achieve the desired correlation. Clearly, the solution to this model correlation problem is not unique. The possibility of obtaining the best solution is to a large extent dependent on accurate identification of model errors and proper selection of physical parameters that model these local regions. In Ref. 11, a strategy using residual force vectors is outlined to locate the errors in the finite element model. A nonzero element in the residual force vector is used in identifying modeling errors.

In this work, both visual comparison of analysis and test measured mode shapes and energy checks are used in identifying the regions of the analytical model (or the components of the spacecraft structure) that participate most in the vibration modes of interest. Specifically, kinetic energy fractions are computed using the normal modes (in the form of velocity); and a higher value of kinetic energy at a particular degree of freedom indicates higher participation. The kinetic energy fractions are computed using the mode shapes as follows:

$$KE = 0.5\,mv^2$$
$$[KE_{ij}]_{\text{fraction}} = \Phi_{ij}\sum_k M_{ik}\Phi_{kj} \tag{8}$$

where KE_{ij} is the kinetic energy associated with the ith degree of freedom in the jth mode shape, and M_{ik} is the term in the ith row and kth column of the mass matrix. The comparison of the kinetic energy matrix terms KE_{ij} between the calculations using the analysis and test mode shapes provides information about the mass distribution and the modal amplitudes at each degree of freedom. The strain energy of a mode, which is also an important parameter in the description of a mode shape, can be computed as

$$SE = 0.5\,ku^2$$
$$[SE_{ij}]_{\text{fraction}} = \Phi_{ij}\sum_k K_{ik}\Phi_{kj} \tag{9}$$

where SE_{ij} is the strain energy associated with the ith degree of freedom in the jth mode shape. The comparison of strain energy terms SE_{ij} between the calculations using the analysis and test mode shapes provides information on the stiffness distribution at each degree of freedom.

Using these energy checks the differences between the analytical model and the physical structure can be located, and structural parameters that model these local regions can then be identified by the analyst for tuning the model, using the approach outlined in the following section.

V. Parameter Estimation Problem

The task of estimating the structural model parameters to correlate the analytical model modal parameters with the test data is posed as a minimization problem of the general form given as follows.

Find the set of design variables X that

$$\begin{aligned}&\text{Minimize:} && E(\mathbf{X})\\ &\text{Subject to:} && g_j(\mathbf{X}) \le 0, \quad j = 1,\\ & && \quad \text{number of inequality constraints}\\ & && x_i^l \le x_i \le x_i^u\end{aligned} \tag{10}$$

where $E(X)$ is the objective or error function to be minimized, $g_j(X)$ is the set of inequality constraint functions, and x^l and x^u are the bounds on the design variables. For the analysis/test correlation process, this minimization problem is specifically cast in the following form.

Minimize:

$$E(X) = \sum_{i=1}^{nfreq}\left\{\left(\frac{\lambda_{t_i}-\lambda_{a_i}}{\lambda_{t_i}}\right)^t [W]\left(\frac{\lambda_{t_i}-\lambda_{a_i}}{\lambda_{t_i}}\right)\right\}$$

Subject to:

a) constraints on diagonal terms of cross-orthogonality matrix

$$1.0 - \frac{\text{abs}[C_x(i,i)]}{0.9} \le 0; \qquad i = 1, n\,\text{freq} \tag{11a}$$

b) constraints on off-diagonal terms of the cross-orthogonality matrix

$$\frac{\text{abs}[C_x(i,j)]}{0.1} - 1.0 \le 0; \qquad i \ne j \tag{11b}$$

c) bounds on the design variables X (11c)

where λ_t and λ_a are the test and analysis eigenvalues, and $[W]$ is the matrix of weighting functions.

To minimize the computational effort required for solving the minimization problem defined by Eqs. (11), an approximate problem using linearized eigenvalue and eigenvector responses is generated and solved.[12] The specific form of linearization used here is the hybrid Taylor series linearization.[13] The overall solution to the minimization problem is obtained by solving a sequence of linearized subproblems as defined by Eqs. (12).

Minimize:

$$E(X) = \sum_{i=1}^{nfreq}\left\{\left(\frac{\lambda_{t_i}-\tilde{\lambda}_{a_i}}{\lambda_{t_i}}\right)^T [W]\left(\frac{\lambda_{t_i}-\tilde{\lambda}_{a_i}}{\lambda_{t_i}}\right)\right\}$$

Subject to:

a) constraints on diagonal terms of cross-orthogonality matrix

$$1.0 - \frac{\text{abs}[\tilde{C}_x(i,i)]}{0.9} \le 0; \qquad i = 1, n\text{freq} \tag{12a}$$

b) constraints on off-diagonal terms of the cross-orthogonality matrix

$$\frac{\text{abs}[\tilde{C}_x(i,j)]}{0.1} - 1.0 \le 0; \qquad i \ne j \tag{12b}$$

c) bounds on the design variables X (12c)

where

$$\tilde{\lambda}_{a_i} = \lambda_{a_i}(X^0) + \sum_{j=1}^{j=ndv} B_j\left(\frac{\partial\lambda_{a_i}}{\partial X_j^0}\right)(X_j - X_j^0)$$

$$B_j = 1 \qquad \text{if} \qquad X_j^{0*}\frac{\partial\lambda_{a_i}}{\partial X_j} > 0$$

$$B_j = \frac{X_j^0}{X_j} \qquad \text{if} \qquad X_j^{0*}\frac{\partial\lambda_{a_i}}{\partial X_j} \le 0$$

$$\tilde{C}_x = f(\tilde{\phi}_A, M_A, \phi_T)$$

$$\tilde{\phi}_{A_{ik}} = \phi_{A_{ik}}(X^0) + \sum_{j=1}^{j=ndv} B_j\left(\frac{\partial\phi_{A_{ik}}}{\partial X_j^0}\right)(X_j - X_j^0)$$

where i is the ith mode shape, the kth degree of freedom, and

$$B_j = 1 \quad \text{if} \quad X_j^{0*}\frac{\partial \phi_{A_{ik}}}{\partial X_j} > 0$$

$$B_j = \frac{X_j^0}{X_j} \quad \text{if} \quad X_j^{0*}\frac{\partial \phi_{A_{ik}}}{\partial X_j} \le 0$$

The method of feasible directions algorithm, programmed in the numerical optimization code Automated Design Synthesis (ADS)[14] is used for solving the constrained minimization problem defined by Eqs. (12).

VI. Modal Parameter Sensitivity Analysis

The sensitivities of the eigenvalues and eigenvectors with respect to the structural model parameters are used to generate the linearized design model, which is in turn used to sequentially move toward the optimum. The gradients are also used in solving the constrained minimization problem, outlined in the previous section.

For a particular eigenvalue λ_j and the corresponding mode shape $\{\phi_j\}$ it is known from the real, symmetric eigenproblem that

$$[K]\{\phi_j\} = \lambda_j[M]\{\phi_j\} \tag{13}$$

with mass orthonormalization

$$\{\phi_j\}[M]\{\phi_j\} = 1 \tag{14}$$

$$\{\phi_j\}^T[M]\{\phi_k\} = 0; \qquad j \neq k \tag{15}$$

The derivative of the jth eigenvalue with respect to the ith design variable is computed as

$$\frac{\partial \lambda_j}{\partial x_i} = \phi_j^T\left[\frac{\partial K}{\partial x_i} - \lambda_j\frac{\partial M}{\partial x_i}\right]\phi_j \tag{16}$$

The derivative of the eigenvectors is a more tedious task and three different methods, including the finite difference equation, Fox's modal method,[15] and the iterative modal method,[16] are implemented and used in this study.

The forward finite difference method requires that the entire structural analysis be repeated for a perturbed variable to compute the derivative of the response. The perturbation step size may affect the accuracy of the sensitivities computed using the finite difference equation. Figure 2 shows a component of the eigenvector response for different perturbations. Clearly, a discontinuity is noticed for perturbation step sizes of 1.0% and above the base design variable value.

With the Fox's modal method, the eigenvector sensitivities are expressed as a linear combination of baseline mode shapes

$$\frac{\partial \phi_j}{\partial x_i} = \sum_{k=1}^{N} C_{jk}\phi_k \tag{17}$$

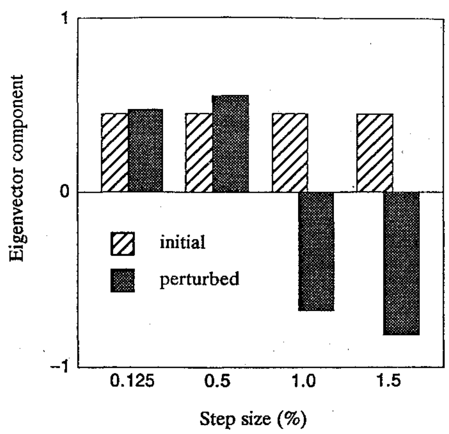

Fig. 2 Eigenvector response for different perturbations (step sizes).

where N is the number of modes used in the expansion. In this study one-fourth of the total number of modes is used for N to compute the derivatives. The coefficients C_{jk} are computed as follows:

$$C_{jk} = \phi_k^T\left(\frac{\partial K}{\partial x_i} - \lambda_j\frac{\partial M}{\partial x_i}\right)\phi_j \bigg/ (\lambda_j - \lambda_k), \qquad j \neq k \tag{18}$$

$$C_{jj} = -\frac{1}{2}\phi_j^T\frac{\partial M}{\partial x_i}\phi_j \tag{19}$$

Although the Fox's modal method is relatively inexpensive, it suffers from inaccuracies when a reduced number of mode shapes is used with the expansion in Eq. (17).

With the iterative modal method, the eigenvector derivative with respect to the ith design variable is obtained by solving

$$[K_0][\Delta\phi_i] = [M_0][\Delta\phi_i][\lambda_0] + [F]$$

where

$$[F] = [M_0][\phi_0][\Delta\lambda_i] + [\Delta M_i][\phi_0][\lambda_0] - [\Delta K_i][\phi_0] \tag{20}$$

where the subscripts 0 and i denote the baseline values and the derivative with respect to the ith design variable, respectively. The only unknown is the derivative of the eigenvector $\Delta\phi_i$ and this is solved for iteratively. The initial values for $\Delta\phi_i$ are the vectors calculated by Fox's modal method and is given by Eq. (17). The convergence of the algorithm is based on a measure of error given by

$$\epsilon_q = \max[\|[K_0][\Delta\phi_i] - [M_0][\Delta\phi_i][\lambda_0] - [F]\|^2] < 0.0001 \tag{21}$$

This method of solving for the eigenvector derivatives requires only a single decomposition regardless of the number of design variables or eigenvectors in the problem.

VII. Methodology Implementation

The systematic identification methodology for correlating the analytical model and test modal parameters outlined in this paper is currently being implemented in the spacecraft analysis/test correlation using design sensitivity (SATCORDS) code. SATCORDS uses MSC/Nastran solution 63 or solution 200 for normal modes analysis, and Nastran direct matrix abstraction programming (DMAP) for self and cross orthogonality, energy fractions, modal effective weight, and iterative modal method-based sensitivity calculations. A flowchart of the analysis/test correlation process is shown in Fig. 3 and a detailed flow of the parameter estimation stage is provided in Fig. 4.

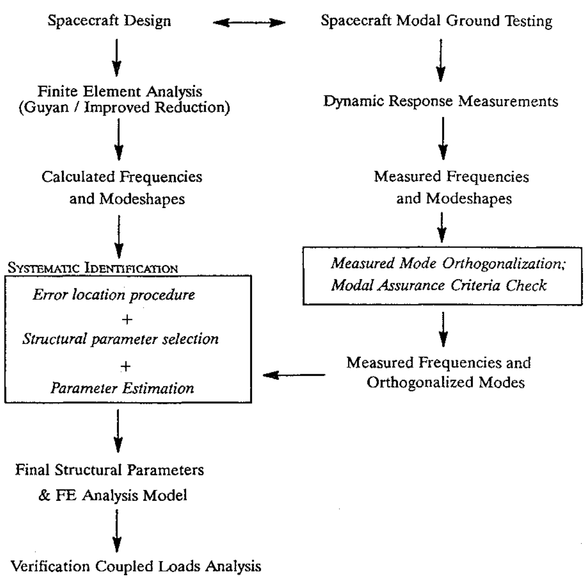

Fig. 3 Analysis/test correlation for spacecraft structures.

Table 1 Kinetic energy fractions for spacecraft primary modes

No.	Mode description	Max energy fraction Test	Max energy fraction Analysis	Location (degree of freedom) Test	Location (degree of freedom) Analysis
1	S/C X bending	0.270	0.248	Center str.	Center str.
2	S/C Y bending	0.326	0.316	Center str.	Center str.
3	Torsion	0.136	0.313	Antivelocity sun panel	GRS canister
4	Anitvel. sun panel, vel. space panel	0.094	0.582	Antivelocity sun panel	RCS tank
5	Vel. space panel, antivel. sun panel	0.182	0.213	Velocity space panel	Velocity space panel
6	S/C Z thrust	0.069	0.356	RCS tank	GRS canister
7	S/C X bending (2nd)	0.089	0.212	Antivelocity space panel	Antivelocity sun panel
8	Antivel. space panel, RCS tank	0.122	0.235	RCS tank, AV space panel	RCS Tank, PMIRR

Table 2 Comparison of frequencies of spacecraft structure

Mode no.	Test frequency, Hz	Analytical model frequency, Hz Precorrel.	Error %	Postcorrel.	Error %
1	18.439	18.00	2.4	18.98	2.9
2	20.234	19.566	3.3	20.48	1.2
3	30.021	27.62	8.0	28.57	4.8
4	34.904	30.544	12.5	33.44	4.2
5	35.665	31.696	11.1	35.76	0.2
6	36.871	32.268	12.5	37.67	2.1
7	39.712	33.411	15.8	40.00	0.7
8	42.361	35.16	17.0	43.15	1.8

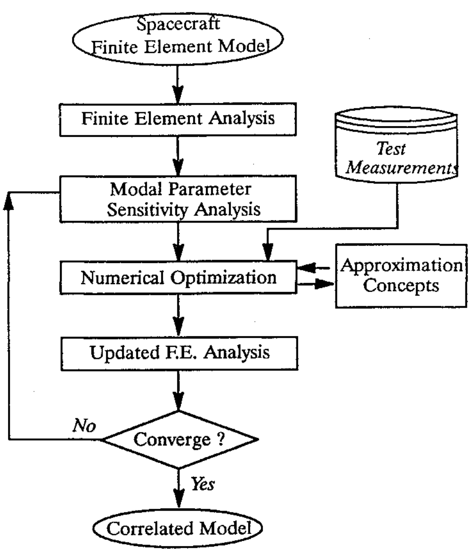

Fig. 4 Flow of the parameter estimation phase.

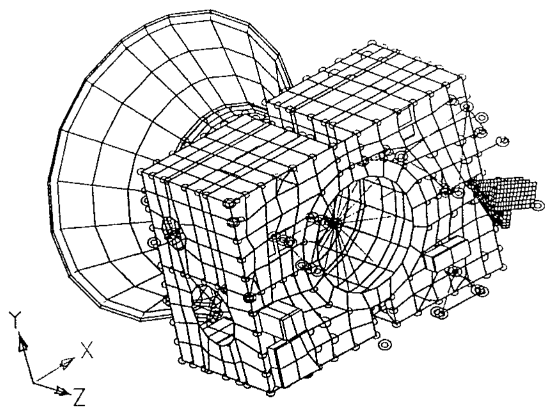

Fig. 5 Spacecraft finite element model.

VIII. Design Example—Spacecraft Structure

The spacecraft model, shown in Fig. 5, is used as the example for the systematic identification methodology outlined in this paper. A Nastran finite element analysis of the spacecraft model is first performed to evaluate the frequencies and mode shapes. Table 2 provides a comparison of these precorrelated model frequencies and test measurements. A DMAP procedure is then executed to compute the modal energy fractions, modal effective weights, and the analysis and test mode shape cross-orthogonality matrix. The test mode shapes are input to this DMAP procedure. The first eight modes, each with a modal effective weight of over 5% of the spacecraft weight, were identified as the primary modes for the analytical model correlation with the measurements. A comparison of the test and precorrelated model energy fractions for each of these eight primary modes, at all of the measurement degrees of freedom, is then performed to identify regions of the spacecraft analytical model that need to be modified. Table 1 provides a comparison of the maximum kinetic energy fraction and its corresponding location (degree of freedom), of the test and pre-correlated model, for each of the eight primary modes. Based on the comparison of energy fractions, a total of 15 independent parameters, representing the various components of the spacecraft system, were identified as design variables for the parameter estimation problem. These parameters include several honeycomb panel skin thicknesses, tank and engine strut areas and inertias, and material modulus and stiffness of springs which model the panel connections. These selected parameters are varied within a manufacturing tolerance range during the parameter estimation phase. In addition, a few modeling omissions between the design drawings and the precorrelated finite element model, which were located based on the energy checks, were also corrected during the correlation process. After six iterations of the parameter estimation scheme, shown in Fig. 4, an acceptable level of correlation was obtained. The parameter estimation problem was solved with and without including the constraints on the mode shape cross-orthogonality requirements. Tables 2–4 provide a comparison

Table 3 Comparison of pre- and postcorrelated mode shape cross-orthogonality matrices

Matrix A: Precorrelated mode shape cross-orthogonality matrix

$$\begin{bmatrix} 0.99 & 0.05 & 0.02 & 0.00 & 0.00 & -0.05 & 0.02 & 0.00 \\ -0.08 & 0.99 & 0.01 & 0.02 & -0.02 & 0.01 & 0.03 & -0.01 \\ -0.03 & -0.01 & 0.93 & 0.22 & -0.16 & -0.05 & 0.06 & 0.13 \\ -0.02 & -0.01 & 0.25 & -0.38 & 0.14 & 0.49 & 0.15 & 0.04 \\ -0.01 & 0.00 & -0.12 & -0.11 & -0.87 & -0.11 & 0.21 & 0.14 \\ -0.03 & -0.02 & -0.17 & 0.35 & 0.11 & 0.02 & 0.26 & 0.34 \\ -0.02 & 0.01 & 0.09 & -0.67 & 0.14 & -0.50 & 0.11 & -0.02 \\ -0.03 & -0.02 & -0.02 & 0.31 & 0.15 & -0.33 & 0.32 & -0.14 \end{bmatrix}$$

Matrix B: Postcorrelated mode shape cross-orthogonality matrix (without mode shape constraints in parameter estimation problem)

$$\begin{bmatrix} 0.99 & -0.02 & -0.01 & 0.00 & 0.00 & 0.04 & 0.00 & 0.01 \\ -0.06 & 0.99 & 0.00 & 0.00 & -0.02 & 0.00 & 0.02 & -0.03 \\ 0.02 & -0.01 & -0.98 & -0.07 & 0.09 & -0.04 & -0.04 & -0.02 \\ -0.01 & 0.00 & 0.05 & 0.07 & 0.91 & 0.24 & -0.13 & -0.01 \\ 0.00 & 0.00 & -0.07 & 0.96 & -0.12 & 0.08 & 0.03 & 0.02 \\ 0.00 & 0.00 & 0.01 & 0.11 & 0.25 & -0.92 & 0.01 & 0.14 \\ 0.01 & 0.00 & 0.03 & 0.03 & -0.11 & -0.07 & -0.92 & 0.06 \\ 0.00 & 0.00 & -0.01 & -0.09 & -0.16 & 0.19 & -0.12 & 0.63 \end{bmatrix}$$

Matrix C: Postcorrelated mode shape cross-orthogonality matrix (with mode shape constraints in parameter estimation problem)

$$\begin{bmatrix} 0.99 & 0.03 & 0.01 & 0.00 & 0.00 & -0.04 & 0.01 & -0.01 \\ -0.06 & 0.99 & -0.03 & 0.03 & -0.02 & 0.00 & 0.03 & -0.02 \\ 0.02 & -0.04 & -0.98 & 0.13 & 0.01 & 0.00 & -0.02 & 0.00 \\ -0.01 & -0.02 & 0.14 & 0.90 & -0.38 & 0.08 & 0.05 & -0.02 \\ 0.00 & -0.01 & 0.04 & 0.32 & 0.84 & 0.23 & -0.10 & 0.01 \\ 0.00 & -0.01 & 0.02 & -0.15 & -0.20 & 0.90 & 0.12 & 0.00 \\ 0.01 & 0.01 & 0.01 & -0.06 & -0.13 & 0.12 & -0.84 & -0.11 \\ 0.00 & -0.01 & 0.02 & 0.06 & -0.09 & 0.00 & -0.21 & 0.89 \end{bmatrix}$$

Table 4 MEW comparison between test and postcorrelated model

		Model effective weight					
	Mode	X,%	Y,%	Z,%	RX,%	RY,%	RZ,%
1	Analysis	35.0	< 1.0	< 1.0	< 1.0	82.1	1.2
	Test	34.2	< 1.0	< 1.0	< 1.0	81.1	< 1.0
2	Analysis	< 1.0	47.6	< 1.0	86.1	< 1.0	< 1.0
	Test	< 1.0	47.8	< 1.0	86.4	< 1.0	< 1.0
3	Analysis	< 1.0	< 1.0	< 1.0	< 1.0	< 1.0	66.7
	Test	< 1.0	< 1.0	< 1.0	< 1.0	< 1.0	58.9
4	Analysis	< 1.0	< 1.0	< 1.0	< 1.0	< 1.0	1.8
	Test	< 1.0	< 1.0	4.7	< 1.0	< 1.0	12.4
5	Analysis	< 1.0	< 1.0	2.4	< 1.0	< 1.0	10.1
	Test	2.3	< 1.0	1.6	< 1.0	< 1.0	5.1
6	Analysis	3.9	2.3	34.8	< 1.0	< 1.0	< 1.0
	Test	1.1	1.1	36.8	< 1.0	< 1.0	< 1.0
7	Analysis	23.3	< 1.0	3.4	< 1.0	6.8	< 1.0
	Test	17.7	< 1.0	2.9	< 1.0	5.6	< 1.0
8	Analysis	< 1.0	< 1.0	6.2	< 1.0	< 1.0	< 1.0
	Test	< 1.0	2.6	5.8	< 1.0	< 1.0	< 1.0

of the frequencies, mode shape cross orthogonality, and modal effective weight of the precorrelated model, postcorrelated model, and test data.

IX. Discussion of Results

Two different parameter estimation problems are solved: first, without imposing any requirements on the mode shapes correlation and, second, with constraints on the terms of the mode shape cross-orthogonality matrix. In both instances, the postcorrelated model frequencies for the eight primary modes of the spacecraft are within the desired ±5% range of the measured frequencies. However, the postcorrelated model/test mode shapes cross-orthogonality matrix (see matrix B of Table 3) for the unconstrained parameter estimation problem has unacceptable diagonal terms for the fourth, fifth, and eighth primary modes. A switch in the locations of the fourth and fifth postcorrelated model mode shapes with respect to the test mode shapes is seen from columns 4 and 5 of matrix B. In the second case, when constraints are imposed on the cross-orthogonality matrix terms, significant improvements are seen in diagonal terms corresponding to the fourth, fifth, and eighth primary modes (see matrix C of Table 3). For all of the diagonal terms, acceptable values of close to or higher than $|0.85|$ are obtained. It is important to note that the off-diagonal terms of matrix C, corresponding to location $C(4, 5)$ and $C(5, 4)$ are comparatively higher than the desired value of $|0.15|$. The reason for these high off-diagonal terms is that both modes 4 and 5 correspond to the same subcomponent (see Table 1 for mode shape description), and are essentially very similar modes.

Using the constrained problem formulation that accounts for both frequency and mode shapes requirements, good correlation of frequencies and mode shapes are obtained between the analysis model predictions and test measurements. It is useful to point out that before performing the automated parameter estimation (or model tuning) phase, it is worthwhile to plot and compare the analytical model and test measured mode shapes. This task can be time consuming; however, it provides a good understanding of the model, specifically the connections, and possibly helps to correct any modeling errors that cannot be performed using the sensitivity-based parameter estimation algorithm.

Both the Guyan and improved reduction procedures are investigated for reduction of the finite element model matrices to the sensor set. With the improved reduction procedure, the orthogonality of the exact mode shapes (full set model mode shape partitioned to the sensor set) with the reduced set model mode shape did not improve compared to the Guyan reduction procedure and, therefore, the Guyan procedure is used for post-test correlation.

Present focus is on considering a more rigorous formulation of the parameter estimation problem and is stated as follows:

Minimize:

$$E(X) = \sum_{i=1}^{n\text{freq}} \left\{ \left(\frac{\lambda_{t_i} - \lambda_{a_i}}{\lambda_{t_i}} \right)^t [W] \left(\frac{\lambda_{t_i} - \lambda_{a_i}}{\lambda_{t_i}} \right) \right\}$$

$$+ \sum_{i=1}^{n\text{freq}} \left\{ \left[\frac{\sqrt{\sum_{j=1}^{n\text{dof}} \left(KE_{t_{ij}} - KE_{a_{ij}} \right)^2}}{n\,\text{dof}} \right]^t [W] \right.$$

$$\left. \times \left[\frac{\sqrt{\sum_{j=1}^{n\text{dof}} \left(KE_{t_{ij}} - KE_{a_{ij}} \right)^2}}{n\,\text{dof}} \right] \right\}$$

Subject to:

a) constraints on diagonal terms of cross-orthogonality matrix

$$1.0 - \frac{\text{abs}[C_x(i,i)]}{0.9} \leq 0; \quad i = 1, n\text{freq} \qquad (22a)$$

b) constraints on off-diagonal terms of the cross-orthogonality matrix

$$\frac{\text{abs}[C_x(i,j)]}{0.1} - 1.0 \leq 0; \qquad i \neq j \qquad (22b)$$

c) bounds on the design variables X (22c)

The problem defined by Eqs. (22) now includes the minimization of the kinetic energy fractions for each mode of interest ($1 - n$ freq), in addition to minimizing the differences in eigenvalues.

X. Summary

An efficient methodology for analysis/test correlation of the dynamic characteristics (frequencies and mode shapes) of a structure, specifically, a spacecraft structure, is outlined. This systematic identification methodology uses both a visual comparison of analysis and test measured mode shapes and energy fractions to identify the regions of error in the analytical model. Structural model parameters that affect these erroneous or local regions are then selected, by the analyst, as variables for tuning the analytical model. Numerical optimization methods along with dynamic parameter sensitivities are used for solving the parameter estimation problem. Analysis and measured mode shapes cross-orthogonality requirements are imposed as direct constraints for the estimation problem. These mode shape cross-orthogonality requirements are critical since the correlated spacecraft model mode shapes along with its mass, stiffness, and damping matrices are used by the launch vehicle organization for performing a detailed coupled loads analysis, which verifies the structural integrity of the spacecraft.[17]

The systematic identification methodology proposed here is robust and efficient in that it updates only local regions of the model that are identified as erroneous regions and requires a minimum number of complete finite element analyses to accomplish the model tuning of complex structural (spacecraft) systems. The methodology allows for including the dynamic analyst's knowledge during the correlation process, by having the analyst identify structural parameters that model the erroneous regions of the analytical model.

The benefits of this technology is well understood in that a well-correlated model provides for accurate evaluation of the spacecraft loads and responses and thereby ensures the structural integrity and launch safety.

References

[1]Pilkey, W. D., and Cohen, R. (eds.), *System Identification of Vibrating Structures, Mathematical Models from Test Data*, American Society of Mechanical Engineers, New York, 1972.

[2]Collins, J. D., Hart, G. C., Hasselman, T. K., and Kennedy, B., "Statistical Identification of Structures," *AIAA Journal*, Vol. 12, No. 2, 1974, pp. 185–190.

[3]Eykhoff, P., *System Identification*, Wiley, New York, 1974, pp. 1–27.

[4]Baruch, M., and Bar Itzhack, I. Y., "Optimal Weighted Orthogonalization of Measured Modes," *AIAA Journal*, Vol. 16, No. 4, 1978, pp. 346–351.

[5]Chen, J. C., and Garba, J. A., "Analytical Model Improvement Using Modal Test Results," *AIAA Journal*, Vol. 18, No. 6, 1980, pp. 684–690.

[6]He, J., and Ewins, D. J., "Analytical Stiffness Matrix Correction Using Measured Vibration Modes," *International Journal of Analytical and Experimental Modal Analysis*, Vol. 1, No. 3, 1986.

[7]Flanigan, C. C., "Test/Analysis Correlation of the STS Centaur using Design Sensitivity and Optimization Methods," Proceedings of Fifth International Modal Analysis Conf., London, April 1987.

[8]Martinez, D. R., Red-Horse, J. R., and Allen, J. J., "System Identification Methods for Dynamic Structural Models of Electronic Packages," *Proceedings of the AIAA/ASME/ASCE/AHS/ASC 32nd Structures, Structural Dynamics, and Materials Conference*, AIAA, Washington, DC, 1991, pp. 2336–2343.

[9]Guyan, R. J., "Reduction of Stiffness and Mass Matrices," *AIAA Journal*, Vol. 3, No. 2, 1965, p. 380.

[10]O'Callahan, J., "A Procedure for an Improved Reduced System (IRS) Model," Proceedings of the 7th International Modal Analysis Conf., Las Vegas, NV, Feb. 1989.

[11]Chen, T. Y., and Wang, B. P., "Finite Element Model Refinement using Modal Analysis Data," *Proceedings of the AIAA/ASME/ASCE/AHS/ASC 29th Structures, Structural Dynamics, and Materials Conference*, AIAA, Washington, DC, 1988, pp. 1219–1229.

[12]Schmit, L. A., and Miura, H., "Approximation Concepts for Structural Synthesis," NASA Contractor Rep. 2552, March 1976.

[13]Starnes, J. H., and Haftka, R. T., "Preliminary Design of Composite Wings for Buckling, Stress and Displacement Constraints," *Journal of Aircraft*, Vol. 16, 1979, pp. 564–570.

[14]Vanderplaats, G. N., "Automated Design Synthesis (ADS) User's Manual," Vanderplaats, Miurat Associates Engineering, Goleta, CA, 1991.

[15]Fox, R. L., and Kapoor, M. P., "Rates of Change of Eigenvalues and Eigenvectors," *AIAA Journal*, Vol. 6, No. 12, 1968, pp. 2426–2429.

[16]High, G. D., "An Iterative Method for Eigenvector Derivatives," MacNeal-Schwendler Corporation World Users Conf., MacNeal-Schwendler Corp., Los Angeles, CA, March 1990.

[17]Kodiyalam, S., "Transient Flight Loads Estimation for Spacecraft Structural Design," *Computing Systems in Engineering*, Vol. 6, No. 3, 1994, pp. 275–283.